Magnetic anisotropy of Co^{II}-W^{V} ferromagnet: single crystal and *ab initio* study

Szymon Chorazy, Robert Podgajny[*], Anna M. Majcher, Wojciech Nitek, Michał Rams, Elizaveta

A. Suturina, Liviu Ungur, Liviu F. Chibotaru and Barbara Sieklucka

Supporting Information

I. Structural characterization

Table S1 The selected bond lengths and angles for **1.**
Fig. S1 The symmetrically independent unit with atom labeling scheme for **1**.
Table S2 Ideal and observed dihedral δ and φ angles in $[W(CN)_8]^{3-}$ units of **1.**
Table S3 Results of Continuous Shape Measurements for $[W(CN)_8]^{3-}$ units in **1**.
Table S4 Results of Continuous Shape Measurements for $[CoN_2O_4]^{2+}$ units in **1**.

II. Magnetic characterization

Table S5 Magnetic properties of selected Co^{II}-$[W^{V}(CN)_8]^{3-}$ magnets.
Fig. S2 Monocrystalline *ac* characteristics for **1**.

III. Details of the *ab initio* calculations

Fig. S3 Structure of the calculated fragment of the **Co3** center.
Fig. S4 Structure of the calculated fragment of the **Co2** center.
Table S6 Contractions of the employed basis sets.
Table S7 Spin-Free Energies (CASSCF) and Spin-Orbit Energies (RASSI) of the **Co2** center (cm^{-1}).
Fig. S5 Orientation of the main anisotropy axes in the ground Kramers doublet of **Co2** center. Color scheme: Co - violet, Ta – green, O – red, N – blue, C – grey, H – white.
Table S8. Spin-Free Energies (CASSCF) and Spin-Orbit Energies (RASSI) of the **Co3** center (cm^{-1}).
Fig. S6 Orientation of the main magnetic axes in the ground Kramers doublet of the **Co3** center.

IV. Magnetic structure simulations.

I. Structural characterization

Table S1 The selected bondlengths and angles for **1.**

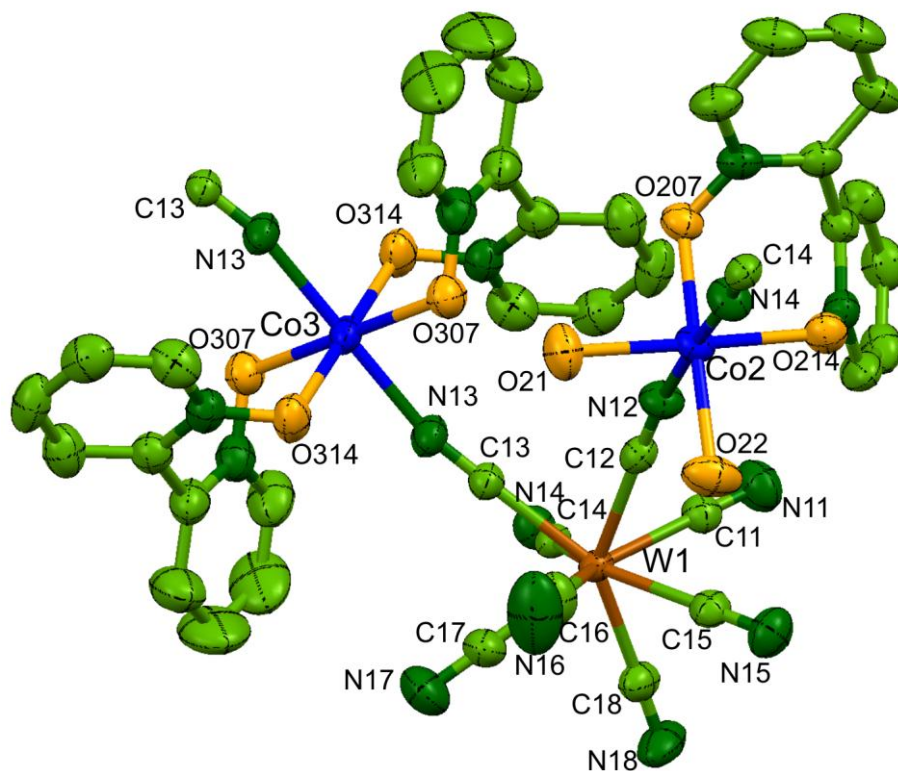| Metal centre			Metal centre		
W1	W-C	2,154-2,180Å	Co2	Co-O207	2,043(2)Å
	C-N	1,140-1,156Å		Co-O214	2,057(2)Å
				Co-O21	2,070(3)Å
	W-C-N	173,7-179,8°		Co-O22	2,138(3)Å
				Co-N14	2,128(3)Å
Co3	Co-O314	2,040(3)Å		Co-N12	2,158(3)Å
	Co-O307	2,092(2)Å			
	Co-N13	2,102(3)Å		Co-N12-C12	154,5(3)°
				Co-N14-C14	175,8(3)°
	Co-N13-C13	178,0(3)°			
				O207-Co-O214	86.20(9)°
	N13-Co-N13	180,0(2)°		O207-Co-O21	92.52(10)°
	O314-Co-O314	180,0(2)°		O214-Co-O21	178.72(11)°
	O307-Co-O307	180,0(2)°		O207-Co-N14	95.48(10)°
				O214-Co-N14	86.72(11)°
	N13-Co-O314	92,83(11)°		O21-Co-N14	93.48(11)°
		87,17(11)°		O207-Co-O22	174.19(10)°
	O314-Co-O307	94,39(10)°		O214-Co-O22	91.55(11)°
		85,61(10)°		O21-Co-O22	89.71(12)°
	O307-Co-N13	95,64(10)°		N14-Co-O22	89.74(11)°
		84,36(10)°		O207-Co-N12	89.66(10)°
				O214-Co-N12	93.87(11)°
				O21-Co-N12	86.04(11)°
				N14-Co-N12	174.86(11)°
				O22-Co-N12	85.14(11)°

Fig. S1 The symmetrically independent unit with atom labeling scheme for **1**. Colors: Co(II) (dark blue), W(V) (brown), carbon atoms (green), nitrogen atoms (dark green), oxygen atoms (yellow). Hydrogen atoms and crystalline water molecules are omitted for clarity. Displacement ellipsoids are drawn at a 60% probability level.

Table S2 Ideal and observed dihedral δ and ϕ angles in $[W(CN)_8]^{3-}$ units of **1**.[S1]

Complex	δ [°]	ϕ[°]
Ideal DD-8	29.5; 29.5; 29.5; 29.5	0
Ideal BTP-8	0; 21.8; 48.2; 48.2	14.1
Ideal SAPR-8	0; 0; 52.4; 52.4	24.5
$[W1(CN)_8]^{3-}$	0.4; 12.1; 47.9; 48.7	21.0 – 23.0

S1 *(a)* E. L. Muetterties and L. J. Guggenberger, *J. Am. Chem. Soc.*, 1974, **96**, 1748-1756; *(b)* D. Visinescu, C. Desplanches, I. Imaz, V. Bahers, R. Pradhan, F. A. Villamen, P. Guionneau and J.-P. Sutter, *J. Am. Chem. Soc.*, 2006, **128**, 10202-10212.

Table S3 Results of Continuous Shape Measurements for $[W(CN)_8]^{3-}$ units in **1**.[S2]

	$[W1(CN)_8]^{3-}$
CSM SAPR-8	0.269
CSM DD-8	1.905
CSM BTP-8	1.508
BTP-8 → SAPR-8	
DevPath	15.9
GenCoord	81.6
SAPR-8 → BTP-8	
GenCoord	34.3
BTP-8 → DD-8	
DevPath	58.2
GenCoord	74.5
DD-8 → BTP-8	
GenCoord	83.7
SAPR-8 → DD-8	
DevPath	12.2
GenCoord	30.6
DD-8 → SAPR-8	
GenCoord	81.7

CSM represent the shape measure relative to the relevant polyhedra: SAPR-8 for the square antiprism, DD-8 for the triangular dodecahedron and BTP-8 for the square face bicapped trigonal prism. Generally, the value of **CSM** is zero, when the analyzed polyhedron exhibits exactly the reference geometry and increases with the degree of distortion. **DevPath** for two polyhedral represents the deviation from the idealized interconversion path between the pair of polyhedra, while **GenCoord** is generalized interconversion coordinates showing the degree of conversion between these polyhedra. The presented set of parameters indicate the dominating SAPR-8 shape of $[W(CN)_8]^{3-}$ in **1**.

S2 M. Llunell, D. Casanova, J. Cirera, M. P. Alemany and S. Alvarez, SHAPE, v. 2.0; Program for the Stereochemical Analysis of Molecular Fragments by Means of Continuous Shape Measures and Associated Tools; Departament de Química Física, Departament de Química Inorganica, and Institut de Química Teorica i Computacional, Universitat de Barcelona: Barcelona, Spain, 2010.

Table S4 Results of Continuous Shape Measurements for $[CoN_2O_4]^{2+}$ units in 1^{S2}

	$[Co2N_2O_4]^{2+}$	$[Co3N_2O_4]^{2+}$
CSM HP-6	31.160	28.374
CSM PPY-6	27.023	27.921
CSM OC-6	0.228	0.327
CSM TPR-6	14.635	16.155
CSM JPPY-5	30.428	31.005

II. Magnetic characterization

Table S5 Magnetic properties of selected samples Co^{II}-$[W^V(CN)_8]^{3-}$ magnets.

Chemical Formula	T_C [K]	M_S [μ_B]	Hysteresis loop (H_C, [Oe])	Ref.
$[Co^{II}_3(DMF)_{12}][W^V(CN)_8]_2$	7.3	10.85	900	S3
$\{Co^{II}_3(H_2O)_6(pyz)_3[W^V(CN)_8]_2\}\cdot 3,5H_2O$	26	8.43	750	S4
$\{Co^{II}_3(H_2O)_4(4,4'-bpy)_3 [W^V(CN)_8]_2\}\cdot 1,5(4,4'-bpy)\cdot 6H_2O$	16	8.17	1200	S4
$([\{Co^{II}(pym)_2\}_2\{Co^{II}(H_2O)_2\}\{W^V(CN)_8\}_2] \cdot 4H2O$	32	8.0	12000[a]	S5
$\{[Co^{II}(H_2O)_2]_3[W^V(CN)_8]_2\}\cdot 4H_2O$	18	8.1	600	S6
$\{Co^{II}(pyr)_4]_2[Nb^{IV}(CN)_8]\}\cdot 4H_2O$[b]	5.9	5.55	80	S7
$[\{Co^{II}(2,2'-bpdo)_2\}\{Co^{II}(2,2'-bpdo)(H_2O)_2\}_2\{W^V(CN)_8\}_3]\cdot 8H_2O$ **1**	6.0	8.72	100[c]	this work

[a]The value observed for mateastable state after irradiatedion at low in SQUID cavity. [b]M_S value corresponds to $Co^{II}_2Nb^{IV}$ composition. [c]The value for monocrystalline sample.

References

S3   D. Li, L. Zheng, Y. Zhang, J. Huang, S. Gao and W. Tang, *Inorg. Chem.*, 2003, **42**, 6123–6129.

S4   R. Podgajny, M. Bałanda, M. Sikora, M. Borowiec, L. Spałek, C. Kapusta and B. Sieklucka, *Dalton Trans.*, 2006, 2801-2809.

S5   S. Ohkoshi, Y. Hamada, T. Matsuda, Y. Tsunobuchi and H. Tokoro, *Chem. Mater.*, 2008, **20**, 3048–3054.

S6   J. M. Herrera, A. Bleuzen, Y. Dromzee, M. Julve, F. Lloret and M. Verdaguer, *Inorg. Chem.*, 2003, **42**, 7052–7059.

S7   D. Pinkowicz, R. Pełka, O. Drath, W. Nitek, M. Bałanda, A. M. Majcher, G. Poneti and B. Sieklucka, *Inorg. Chem.*, 2010, **49**, 7565-7576.
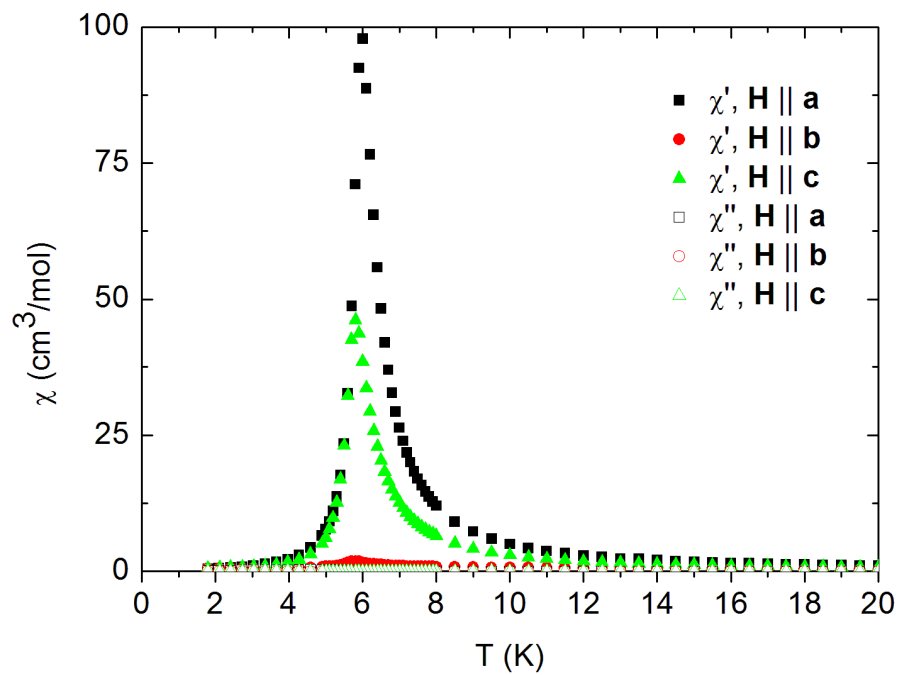
Fig. S2 Monocrystalline *ac* characteristics for **1**.

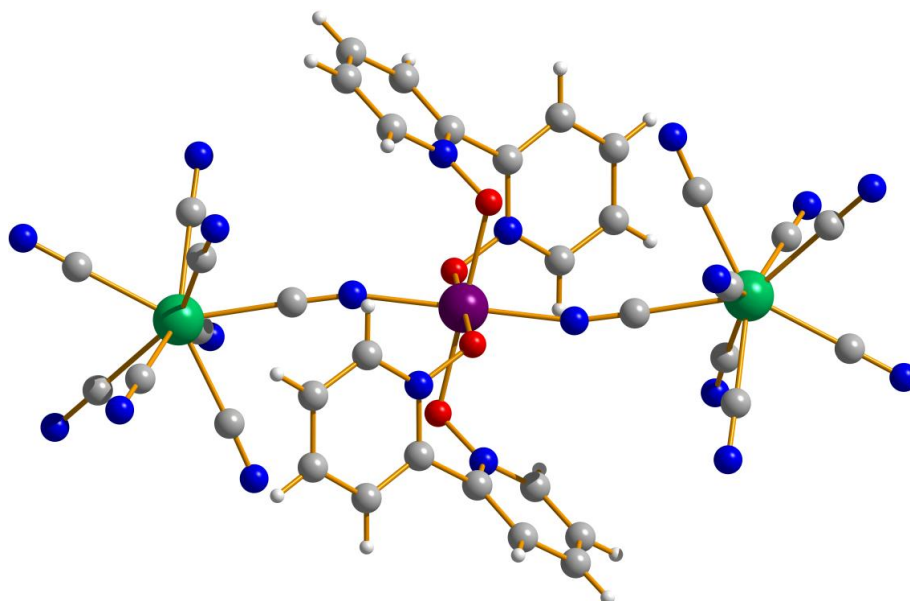## III. Details of the *ab initio* calculations

Fig. S3 Structure of the calculated fragment of the **Co3** center. Color scheme: Co - violet, Ta – green, O – red, N – blue, C – grey, H – white.

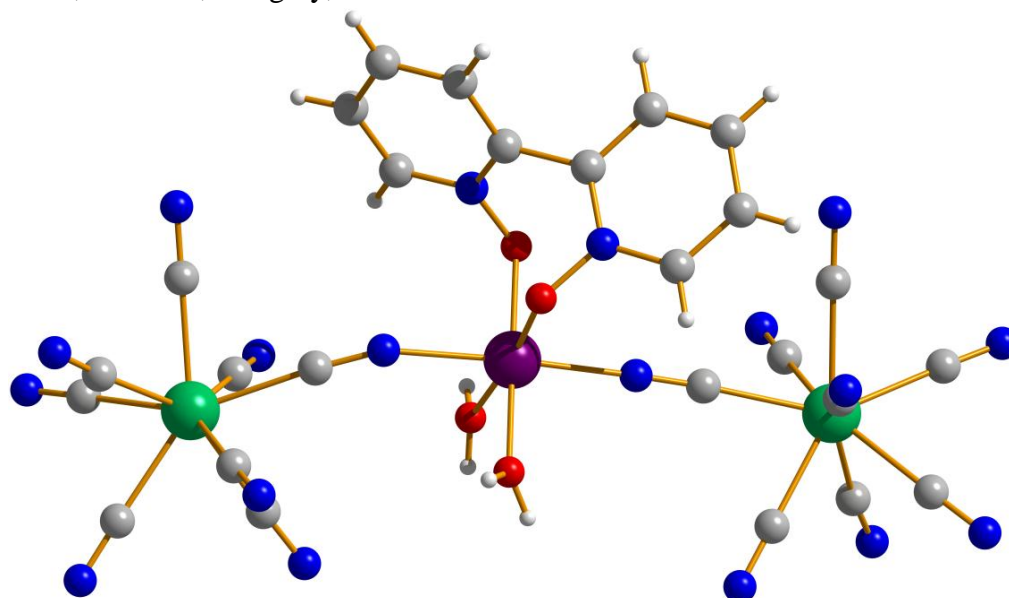**Fig. S4** Structure of the calculated fragment of the Co2 center. Color scheme: Co - violet, Ta – green, O – red, N – blue, C – grey, H – white.

Table S6 Contractions of the employed basis sets.

Basis Sets
Co.ANO-RCC...5s4p2d1f.
Ta.ANO-DK3...6s4p3d1f.
O.ANO-RCC...3s2p.
N.ANO-RCC...3s2p. (close)
N.ANO-DK3...2s1p. (distant)
C.ANO-DK3...2s1p.
H. ANO-DK3...1s.

Table S7 Spin-Free Energies (CASSCF) and Spin-Orbit Energies (RASSI) of the **Co2** center (cm^{-1}).

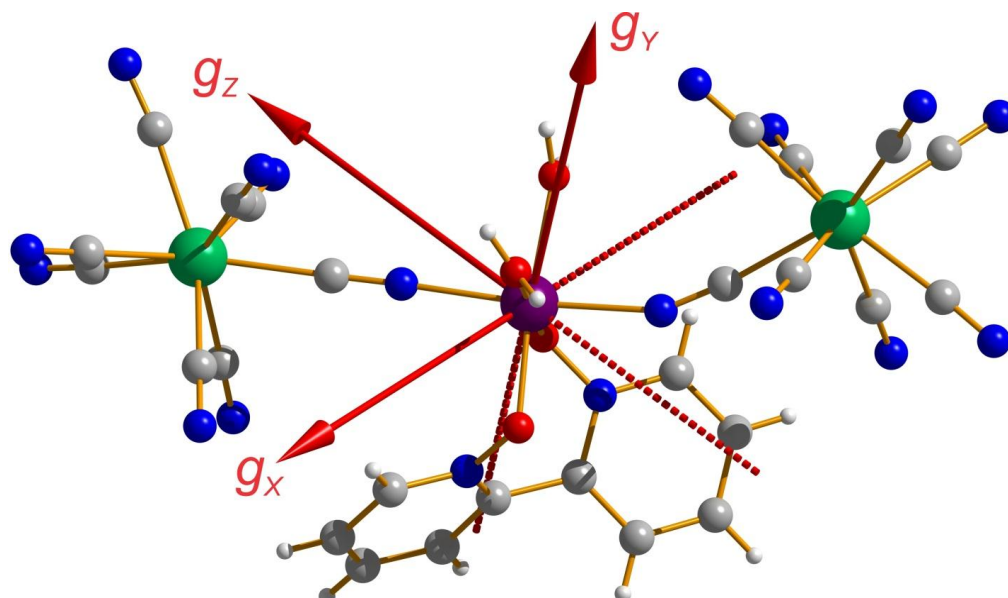| 2S+1		AS1	AS2	AS1	AS2
		CASSCF	CASSCF	RASSI	RASSI
$^4T_1$		**0.000**	**0.000**	0.000	0.000
		509.060	**538.200**	172.535	150.650
		1141.882	**1238.648**	705.107	712.364
		6607.384	7120.222	993.822	963.345
quartets		7144.949	7693.471	1493.650	1540.474
		7292.876	7896.132	1601.691	1640.099
		14608.501	15665.396	6909.480	7381.233
		23224.478	22268.955	6966.507	7430.301
		24220.331	23298.288	7436.171	7948.157
		24723.670	23842.317	7480.133	7988.704
		14699.648	13914.583	7625.347	8178.680
		15646.319	14906.217	7738.914	8275.060
		20072.846	19818.454	14976.851	14191.439
		20174.452	19931.014	14982.279	15179.631
		20436.026	20270.061	15017.289	15984.425
		20608.432	20462.483	15954.990	15987.658
		20882.162	20736.102	20191.237	19920.444
		21162.674	21101.005	20436.676	20190.148
		25093.245	25420.638	20791.032	20571.940
		25951.915	25607.151	21069.025	20841.838
		26187.419	25853.845	21353.775	21151.655
		26346.667	26038.002	21622.531	21502.899
doublets		28737.741	28570.202	23390.158	22429.858
		29119.740	28956.857	23458.026	22482.604
		29360.848	29227.056	24339.762	23422.304
		29669.432	29587.486	24437.085	23499.094
		29809.839	29743.590	24789.997	23936.585
		30082.911	30012.460	25067.269	24152.012
		31688.222	31558.594	25323.620	25524.725
		32150.701	32062.752	26502.353	26070.689
		34593.899	34586.920	26679.251	26259.485
		34679.544	34762.282	27132.584	26788.256
		34840.389	34886.694	29100.721	28899.119
		35269.751	35476.780	29513.838	29303.881
		35734.261	35929.319	29801.041	29619.874
		…	…	…	…

Fig. S5 Orientation of the main anisotropy axes in the ground Kramers doublet of **Co2** center. Color scheme: Co - violet, Ta – green, O – red, N – blue, C – grey, H – white.

Table S8 Spin-Free Energies (CASSCF) and Spin-Orbit Energies (RASSI) of the **Co3** center (cm^{-1}).

2S+1			AS1	AS2	AS1	AS2
			CASSCF	CASSCF	RASSI	RASSI
			0.000	**0.000**	0.000	0.000
	$^4T_1$		**997.252**	**1082.055**	112.973	93.294
			1140.962	**1227.046**	985.384	1045.174
			6481.762	6914.014	1275.686	1307.809
quartets			7189.815	7660.856	1466.810	1504.869
			8309.674	8981.533	1631.697	1667.709
			15062.204	16054.375	6710.107	7103.602
			23494.830	22496.560	6786.461	7169.767
			24192.691	23223.194	7413.302	7846.147
			25204.265	24320.165	7485.935	7911.628
			14168.000	13355.852	8529.857	9161.587
			15830.199	15145.182	8622.825	9242.489
			19516.804	19192.678	14402.695	13559.406
			20113.694	19862.371	15352.467	15344.156
			20439.026	20211.966	15357.403	16294.342
			20673.954	20419.057	16062.026	16299.139
			21034.814	20907.101	19749.957	19400.473
			21442.064	21464.526	20258.194	19985.255
doublets			25275.066	25403.907	20622.849	20356.199
			25788.883	25557.216	21023.212	20727.792
			26061.007	25706.927	21399.445	21217.420
			26264.691	25910.254	21828.935	21784.599
			28930.118	28715.736	23566.723	22574.727
			29249.373	29037.952	23638.297	22627.062
			29411.860	29218.640	24230.080	23272.833
			29922.075	29843.781	24378.854	23389.452
			30214.171	30120.246	25084.426	24276.523

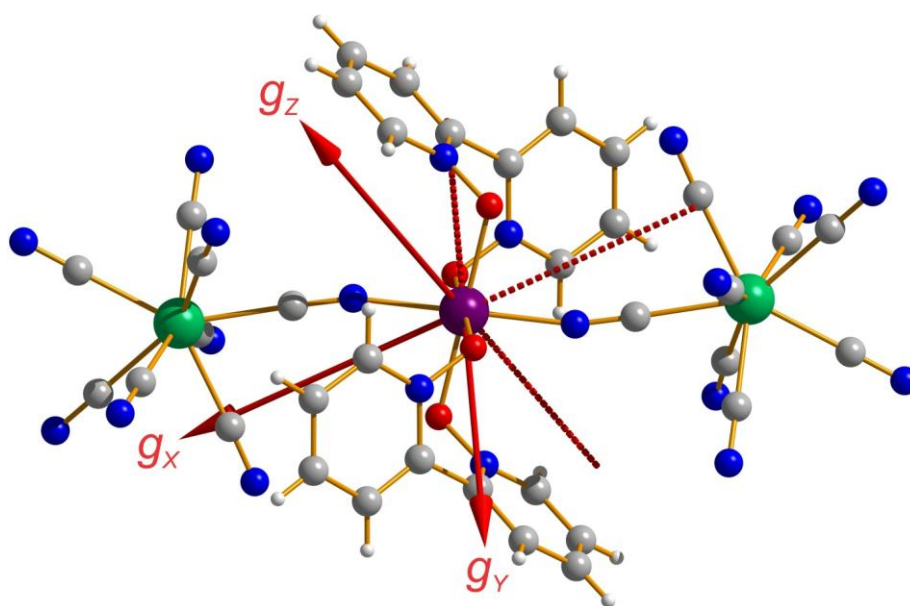|			
30728.819	30744.325	25356.400	24503.302
32108.746	31965.053	25448.290	25517.489
32271.801	32174.320	26338.388	25836.148
34833.411	34798.084	26615.819	26155.683
34973.433	34971.559	26949.127	26593.953
35247.288	35229.155	29171.825	28920.525
35633.236	35792.050	29596.889	29361.415
35740.103	35938.887	29717.021	29476.507
…	…	…	…

Fig. S6 Orientation of the main magnetic axes in the ground Kramers doublet of the **Co3** center. Color scheme: Co - violet, Ta – green, O – red, N – blue, C – grey, H – white.

IV. Magnetic structure simulations

Magnetic structure was simulated using molecular field approach. The energy of the Co_6W_4 unit

$$E = -2\vec{m}_W\vec{h}_W - 2\vec{m}_{W'}\vec{h}_{W'} - 2\vec{m}_{Co2}\vec{h}_{Co2} - 2\vec{m}_{Co2'}\vec{h}_{Co2'} - \vec{m}_{Co3}\vec{h}_{Co3} - \vec{m}_{Co3'}\vec{h}_{Co3'}$$

was minimized. It takes into account two different orientations of Co3 ions, and two different orientations of Co2 ions in the elementary cell. The molecular field

$$\vec{h}_W = \lambda(\vec{m}_{Co2} + \vec{m}_{Co2'} + \vec{m}_{Co3'})$$
$$\vec{h}_{W'} = \lambda(\vec{m}_{Co2} + \vec{m}_{Co2'} + \vec{m}_{Co3})$$
$$\vec{h}_{Co2} = h_{Co2'} = \lambda(\vec{m}_W + \vec{m}_{W'})$$
$$\vec{h}_{Co3} = 2\lambda\vec{m}_{W'}$$
$$\vec{h}_{Co3'} = 2\lambda\vec{m}_W$$

is calculated assuming the same exchange interaction for all Co-W pairs. Two sublattices for W ions is taken into account, because of their Co3 or Co3' neighborhood.

Magnetic moments in the saturation limit (ground state at $T = 0$) are

$$\vec{m}_W = \frac{1}{2}2\frac{\vec{h}_W}{h_W}$$

$$\vec{m}_{Co3} = \frac{1}{2}\hat{R}_{Co3}\hat{g}_{Co3}\hat{R}_{Co3}^{-1}\frac{\vec{h}_{Co3}}{h_{Co3}}$$

etc.

where R are rotation matrices of local axes of Co g-tensors. Isotropic g-tensors for W ions with $g=2.0$ were used. From *ab initio* calculations

$$\hat{R}_{Co3} = \begin{pmatrix} -0.330 & -0.447 & 0.824 \\ 0.912 & 0.077 & 0.423 \\ -0.245 & 0.891 & 0.377 \end{pmatrix} \qquad \hat{R}_{Co2} = \begin{pmatrix} 0.488 & 0.310 & -0.805 \\ -0.853 & -0.031 & -0.540 \\ -0.187 & 0.950 & 0.245 \end{pmatrix}$$

and $g_{Co2} = (2.061, 2.950, 7.301)$, $g_{Co3} = (5.396, 4.819, 2.283)$. R for Co2 and Co3' are reflected in *ac* plane.

These equations are easily solvable (using Mathematica software) after parametrization

$$\frac{\vec{h}_W}{h_W} = (\cos\varphi_W \sin\theta_W, \sin\varphi_W \sin\theta_W, \cos\theta_W)$$

$$\frac{\vec{h}_{W'}}{h_{W'}} = (\cos\varphi_{W'} \sin\theta_{W'}, \sin\varphi_{W'} \sin\theta_{W'}, \cos\theta_{W'})$$

where θ_W ... $\varphi_{W'}$ are four free parameters. The resulting values and orientations of magnetic moments does not depend on the λ molecular field constant; during simulation $\lambda=1$ was used. The magnetization energy has the minimum for $\varphi_W = 0.073$, $\varphi_{W'} = -0.073$, and $\theta_W = 1.118$, and $\theta_{W'} = 1.118$.

Magnetic moments are then equal ($x \parallel a$, $y \parallel b^*$, $z \parallel c$)

	Mx/μ_B	My/μ_B	Mz/μ_B
W	-0.90	-0.07	0.43
W'	-0.90	0.07	0.43
Co3	-1.61	0.52	1.30
Co3'	-1.61	-0.52	1.30
Co2	-2.68	-1.19	1.05
Co2'	-2.68	1.19	1.05
Total/Co_3W_2	-8.76	0.0	4.28

Total magnetization of the crystal along axes: M_a=-8.76, M_{b^*}=0.0, M_c=4.28 μ_B per Co_3W_2 unit. The magnetization cancels along the $b^* \approx b$ direction, which is consistent with the experimental data. It should be stressed that this result was obtained without imposing the crystal glide plane symmetry on the solution (e.g. independent variables for φ_W and $-\varphi_{W'}$ were used in minimization of energy). However, the glide plane symmetry is preserved in this case. The spontaneous magnetization is 9.75 μ_B, within the ac plane, creating 26 deg from the a crystallographic axis.